

Supplementary Information

**Simultaneous bacterial inactivation and degradation of emerging pollutant under visible  
light by ZnFe<sub>2</sub>O<sub>4</sub> co-modified with Ag and rGO**

Nirina Khadgi\*, Akhanda Raj Upreti, Yi Li

Key Laboratory of Integrated Regulation and Resource Development of Shallow Lakes, Ministry  
of Education, College of Environment, Hohai University, Xikang Road #1, Nanjing 210098, P.R.  
China

**Fig. S1:** XRD patterns of (a) GO (b) rGO (c) ZnFe<sub>2</sub>O<sub>4</sub> and (d) ZnFe<sub>2</sub>O<sub>4</sub>/rGO and (e) ZnFe<sub>2</sub>O<sub>4</sub>Ag/rGO.

**Fig. S2:** XPS survey spectrum of typical elements (a) Zn 2p (b) Fe 2p (c) Ag 3d and (e) C 1s of ZnFe<sub>2</sub>O<sub>4</sub>-Ag/rGO NCs.

**Fig. S3.** UV-vis absorbance spectrum of (a) GO (b) ZnFe<sub>2</sub>O<sub>4</sub> (c) ZnFe<sub>2</sub>O<sub>4</sub>/rGO and (d) ZnFe<sub>2</sub>O<sub>4</sub>-Ag/rGO NCs.

**Fig. S4:** Photocatalytic performance of ZnFe<sub>2</sub>O<sub>4</sub>-Ag/rGO NC in different catalyst loadings for (a) *E. coli* inactivation and (b) EE2 degradation.

**Fig. S5:** EE2 degradation during photocatalytic treatment with different catalysts.

**Fig. S6:** UV-vis absorption spectra for EE2 suspension during the degradation process

**Fig. S7:** Change in photoluminescence spectrum indicating •OH production.

**Fig. S8:** Change in absorbance indicating production of O<sub>2</sub><sup>•-</sup>.

**Fig. S9:** Production of H<sub>2</sub>O<sub>2</sub> after different irradiation time.

**Fig. S10:** SEM images of *S. haemolyticus* (a) before addition of nanocomposite, (b) at time 60min, (c) 90 min and (d) Inactivation curve.

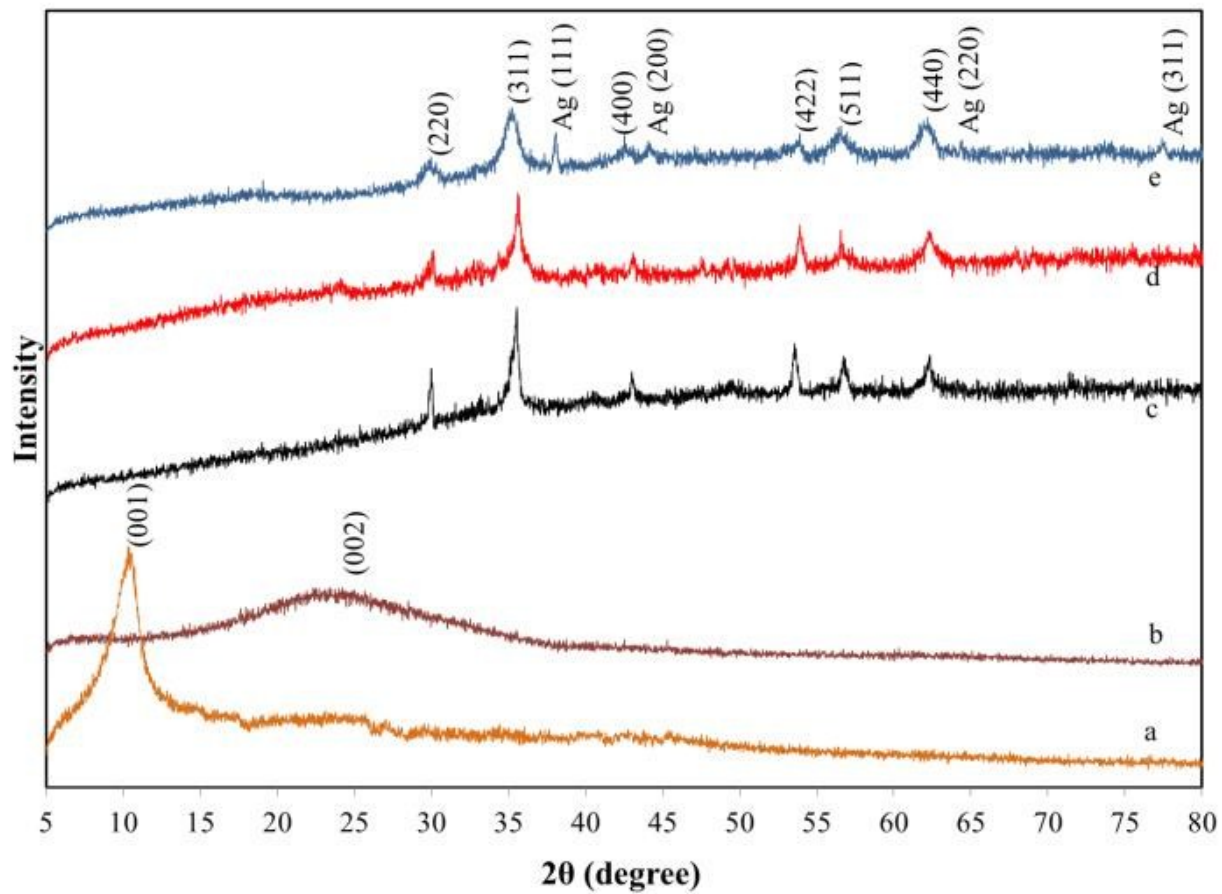
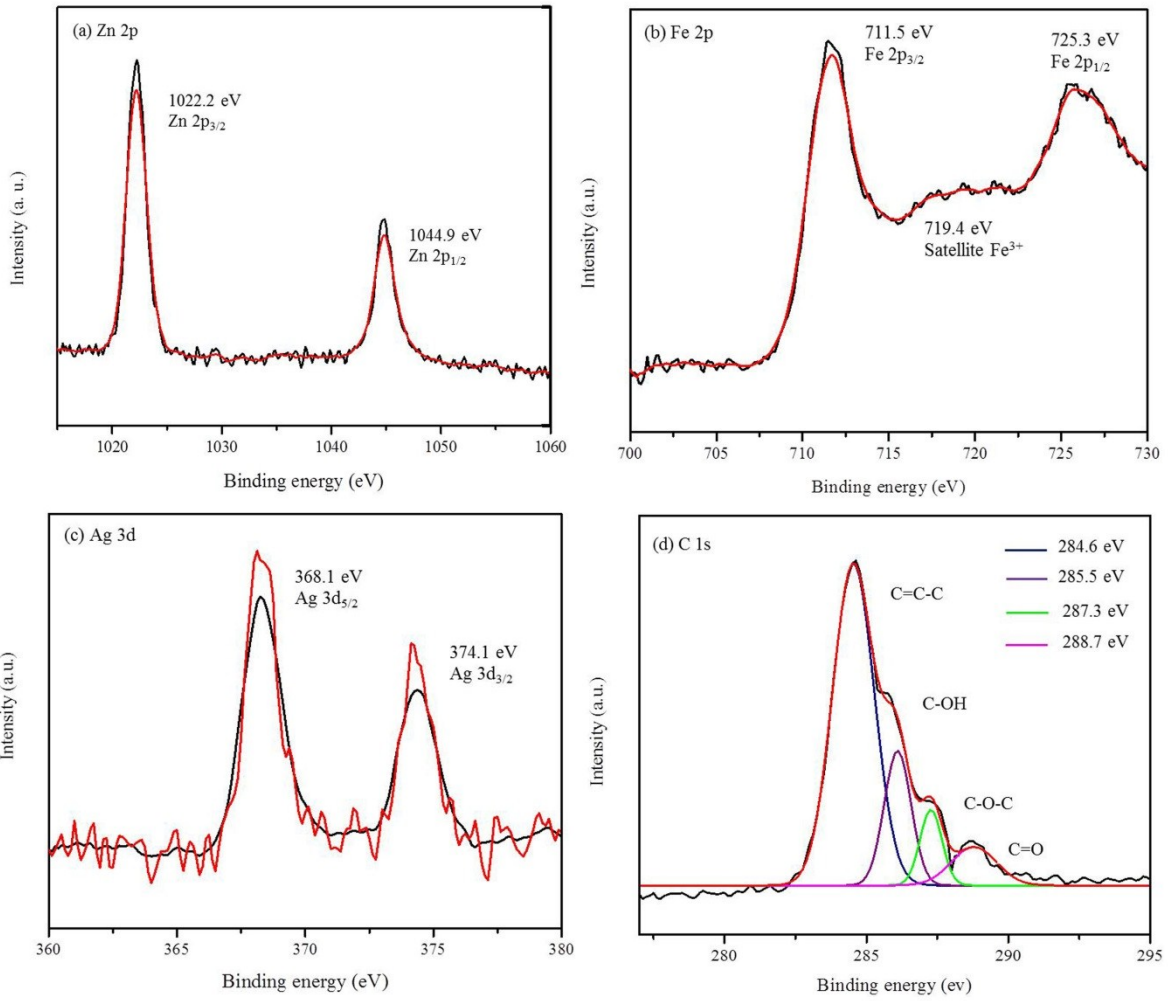


Fig. S 1- XRD patterns of (a) GO (b) rGO (c) ZnFe<sub>2</sub>O<sub>4</sub> and (d) ZnFe<sub>2</sub>O<sub>4</sub>/rGO and (e) ZnFe<sub>2</sub>O<sub>4</sub>Ag/rGO



**Fig. S 2 - XPS survey spectrum of typical elements (a) Zn 2p (b) Fe 2p (c) Ag 3d and (e) C 1s of ZnFe<sub>2</sub>O<sub>4</sub>-Ag/rGO NCs.**

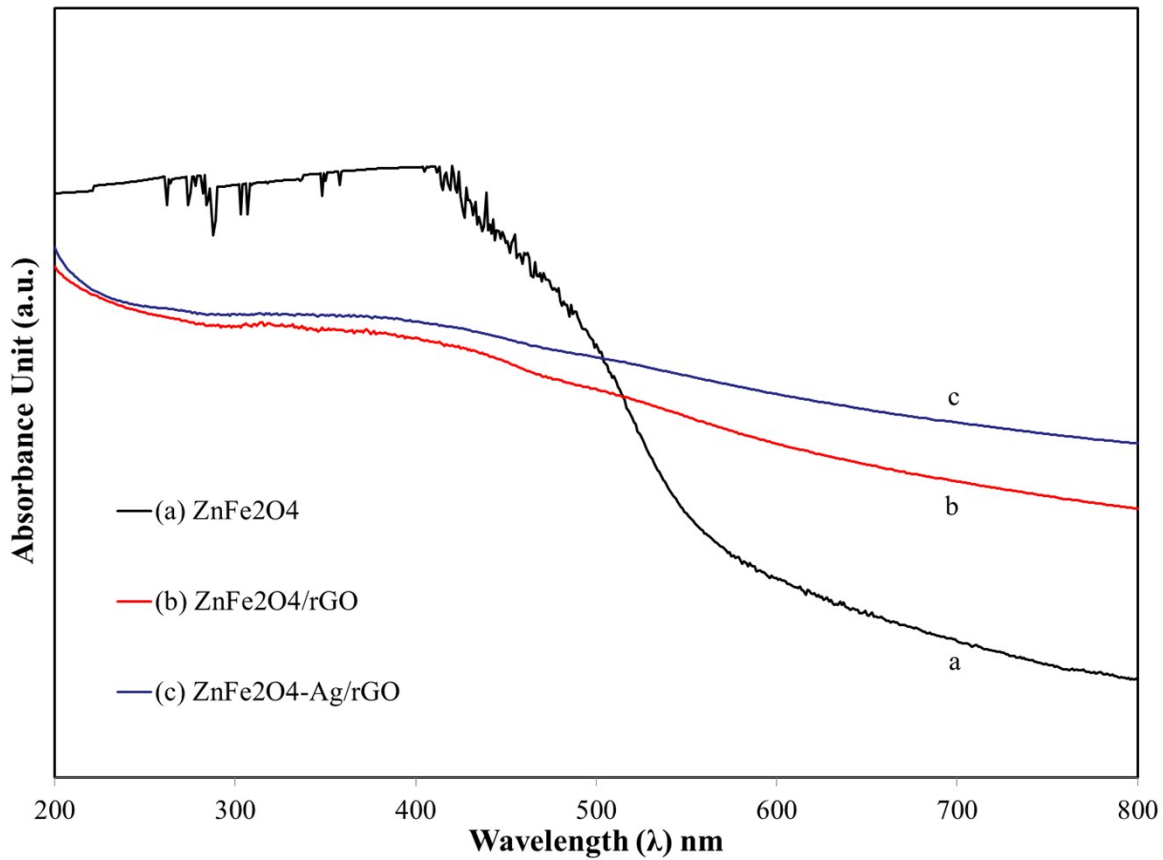


Fig. S 3 - UV- diffuse reflectance spectra of (a) ZnFe<sub>2</sub>O<sub>4</sub> (b) ZnFe<sub>2</sub>O<sub>4</sub>/rGO and (c) ZnFe<sub>2</sub>O<sub>4</sub>-Ag/rGO.

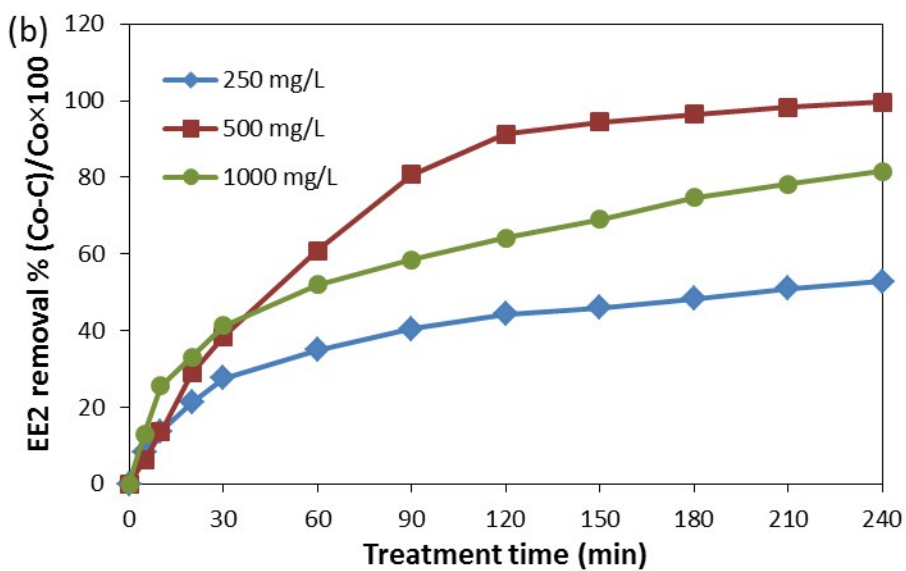
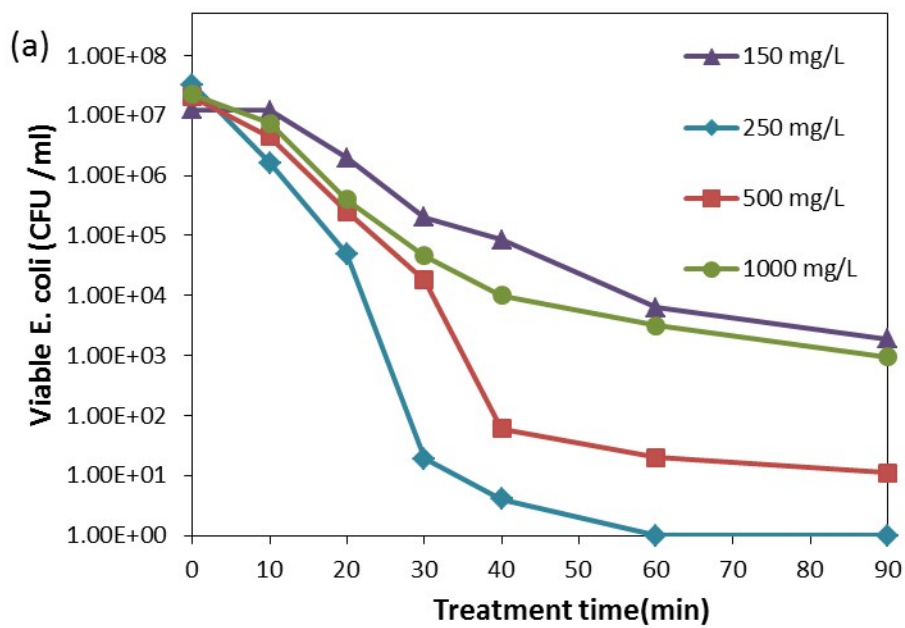


Fig. S 4 - Photocatalytic performance of  $ZnFe_2O_4$ -Ag/rGO NC in different catalyst loadings for (a) *E. coli* inactivation and (b) EE2 degradation.

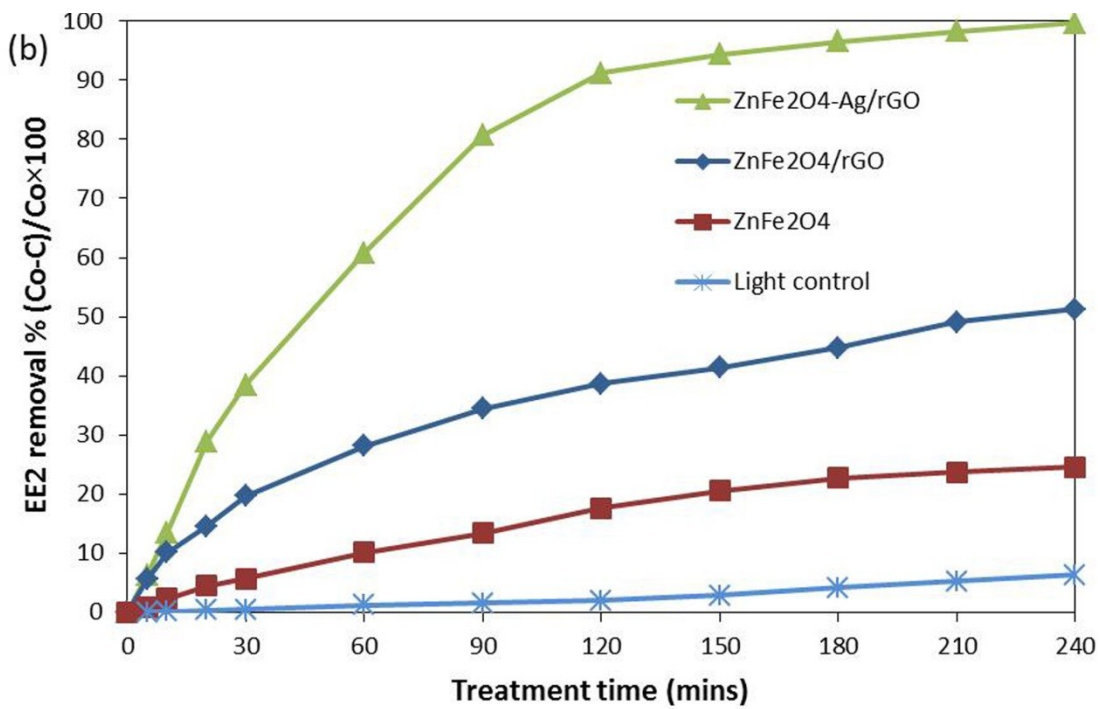


Fig. S 5 - EE2 degradation during photocatalytic treatment with different catalysts.

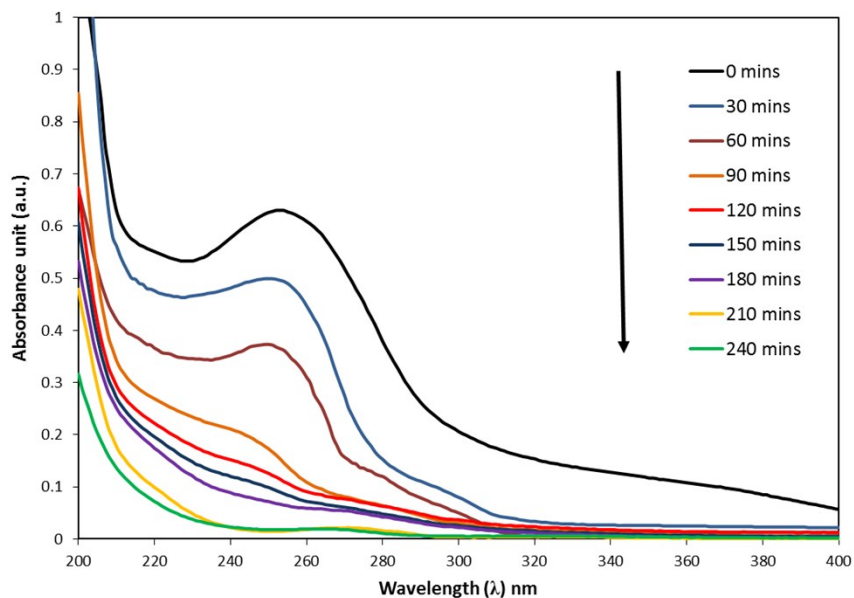


Fig. S 6 - UV-vis absorption spectra for EE2 suspension during the degradation process.

The decrease of the absorption peak with treatment time and appearance of no new absorption peak in the whole spectrum indicates the total degradation of substituted benzene ring of EE2 after 240 min of irradiation [1] The absorption peak 239 and 280 nm indicates the substituted benzene ring of EE2. The absorption around 280 nm indicates the destruction of phenolic ring also responsible for estrogenic activity [2]

**Reference:**

[1] B. Liu, F. Wu and N. S. Deng. UV-light induced photodegradation of 17 $\alpha$ -ethynylestradiol in aqueous solutions. *J. Hazard. Mater.* 98(2003)311–316.

[2] M. G. Maniero, D. M. Bila, M. Dezotti Degradation and estrogenic activity removal of 17 $\beta$ -estradiol and 17 $\alpha$ -ethynylestradiol by ozonation and O<sub>3</sub>/H<sub>2</sub>O<sub>2</sub> *Sci.Total Environ.* 407(2008)105 – 115.

### Detection of ROS ( $\text{OH}^\bullet$ , $\text{O}_2^{\bullet-}$ and $\text{H}_2\text{O}_2$ ) generation

The generation of ROS like  $\text{OH}^\bullet$ ,  $\text{O}_2^{\bullet-}$  and  $\text{H}_2\text{O}_2$ , during the photocatalytic treatment that causes oxidative stress were confirmed using different techniques. The samples withdrawn after every 30 mins of light irradiation were filtered to measure these ROS generation.

The formation of  $\text{OH}^\bullet$  was detected by PL technique using terephthalic acid as a probe molecule [1].  $\text{OH}^\bullet$  radicals produced during the photocatalytic process reacts with terephthalic acid in alkaline solution to produce highly fluorescent, 2-hydroxyterephthalic acid (TAOH). PL spectra of the generated TAOH acid were measured on a Hitachi F-4700 fluorescence spectrophotometer. The intensity of the PL signal was measured at emission wavelength of 425 nm with excitation wavelength at 315 nm. The gradual increase in PL at around 425 nm with increasing irradiation time reveals the production of  $\bullet\text{OH}$  radicals as shown in Fig. S2.

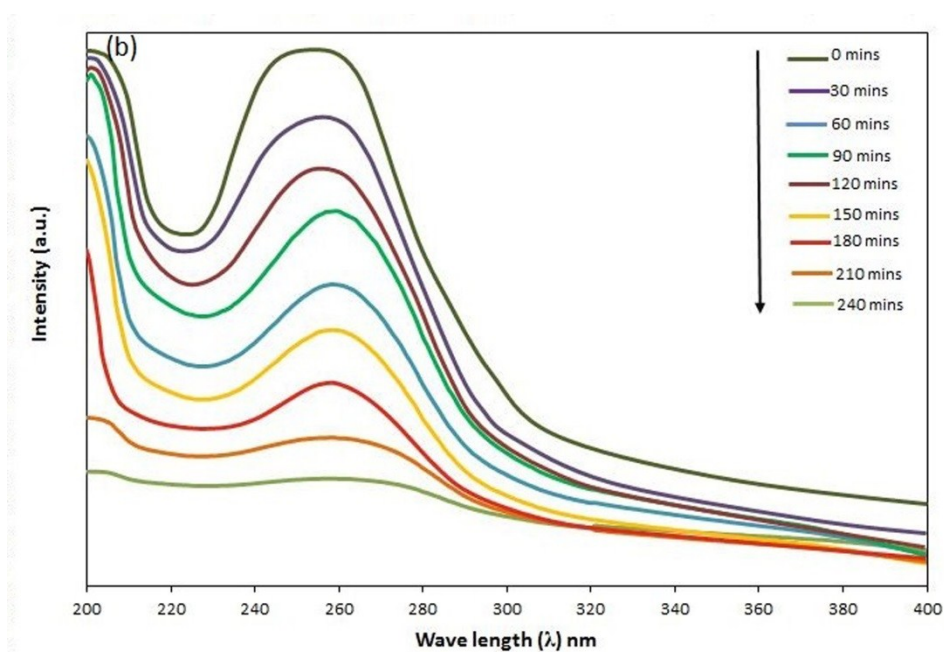


Fig. S 7 - Change in photoluminescence spectrum indicting  $\bullet\text{OH}$  production.

The formation of  $\text{OH}^\bullet$  was detected by PL technique using terephthalic acid as a probe molecule [1]. The generation of  $\text{O}_2^{\bullet-}$  was determined by the nitroblue tetrazolium (NBT) assay [2].  $\text{O}_2^{\bullet-}$  converts the soluble colorless NBT into insoluble purple formazan. Formation of  $\text{O}_2^{\bullet-}$

was confirmed by decrease in the peak at 259 nm suggesting conversion of colourless NBT to insoluble purple formazan by  $O_2^{\bullet-}$  formed during the photocatalytic treatment as shown in Figure S3.

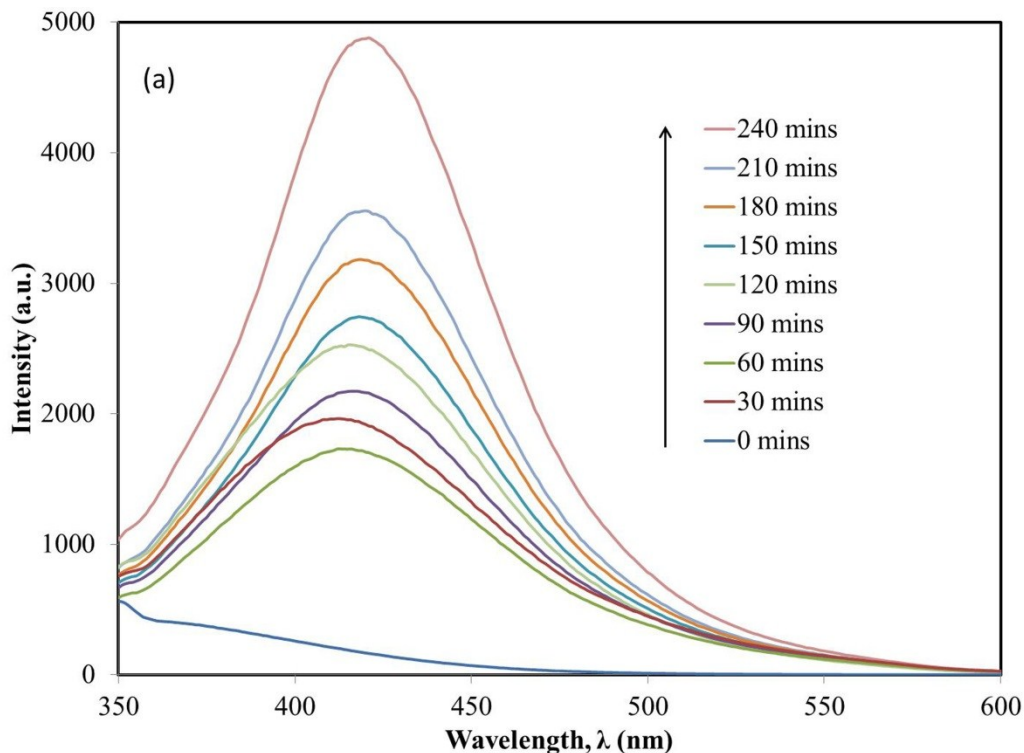
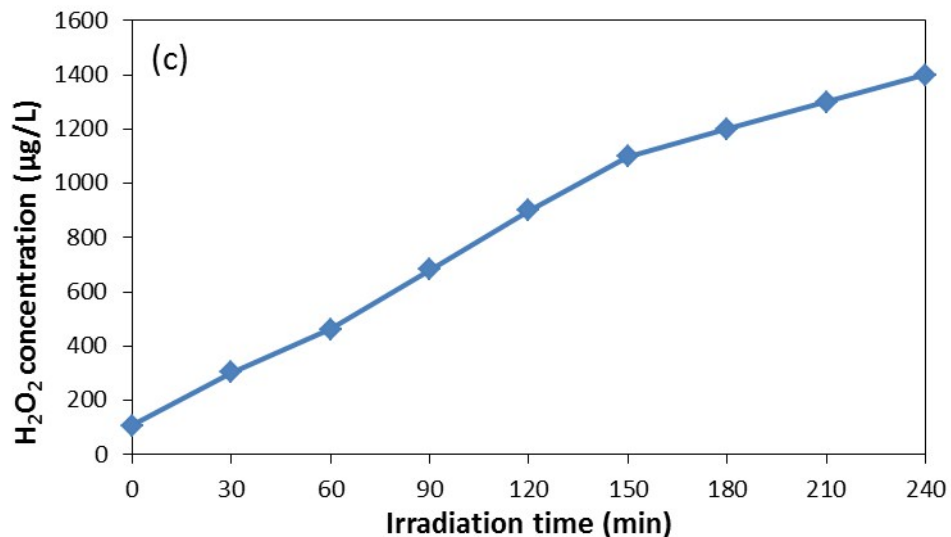


Fig. S 8 - Change in absorbance indicating production of  $O_2^{\bullet-}$ .

The formation of  $OH^{\bullet}$  was detected by PL technique using terephthalic acid as a probe molecule [1]. The generation of  $O_2^{\bullet-}$  was determined by the nitroblue tetrazolium (NBT) assay [2]. The concentration of  $H_2O_2$  was monitored using a titanium (IV) oxysulfate solution via a spectrophotometric method at 410 nm (modified method DIN38402H15) [3]. The production of  $H_2O_2$  was determined by measuring the absorbance of yellow pertitanic acid formed by the reaction between Titanium ions and  $H_2O_2$ , using Titanium Oxysulfate method. The continuous increase in  $H_2O_2$  concentration over the irradiation time is a clear indication of  $H_2O_2$  production.



**Fig. S 9 - Production of H<sub>2</sub>O<sub>2</sub> after different irradiation time**

**References:**

- [1] K. Bubacz, E. Kusiak-Nejman, B. Tryba, A.W. Morawski, Investigation of OH radicals formation on the surface of TiO<sub>2</sub>/N photocatalyst at the presence of terephthalic acid solution. Estimation of optimal conditions. *J. Photochem. Photobiol. A Chem.* 261 (2013) 7-11
- [2] T. Hirakawa and Y. Nosaka, Properties of O<sub>2</sub><sup>•-</sup> and OH<sup>•</sup> Formed in TiO<sub>2</sub> Aqueous Suspensions by Photocatalytic Reaction and the Influence of H<sub>2</sub>O<sub>2</sub> and Some Ions. *Langmuir*, 18 (2002) 3247–3254.
- [3] C. Ruales-Lonfat, N. Benítez, A Sienkiewicz, C. Pulgarín, Deleterious effect of homogeneous and heterogeneous near-neutral photo-Fenton system on Escherichia coli. Comparison with photo-catalytic action of TiO<sub>2</sub> during cell envelope disruption. *Appl. Catal. B: Environ.* 160-161(2014) 286–297.



**Fig. S 10 - Separation of ZnFe<sub>2</sub>O<sub>4</sub>-Ag/rGO NC from the suspension using its magnetic property.**